CrossMark

ORIGINAL PAPER

New bulky side chain substituted benzodithiophene based 2D-conjugated polymers for optoelectronic applications

**Kakaraparthi Kranthiraja[1] · Sang Ho Park[1] ·
Woosum Cho[1] · Won-Tae Park[2] · Yong-Young Noh[2] ·
Sung-Ho Jin[1] · Jae Wook Lee[3]**

Abstract In order to explore the effect of bulky side chain substituted ben-zodithiophene (BDT) based polymers on optoelectronic properties, here we have designed and synthesized two new 2D conjugated donor–acceptor (D–A) copoly-mers **P1** and **P2** via Stille coupling of 2,3-bis(4-(2-ethylhexyloxy)phenyl)thiophene (BAPT) substituted BDT as (D) unit and 1,3-di(2-bromothien-5-yl)-5-(2-ethyl-hexyl)thieno[3,4-c]pyrrole-4,6-dione (TPD) or 2,5-ethylhexyl-3,6-bis(5-bromothio-phen-2-yl)pyrrolo[3,4-c]-pyrrole-1,4-dione (DPP) as (A) units. The new polymers **P1** and **P2** showed broad absorption windows with vibronic shoulders indicate π–π stacking of polymer backbones. In addition **P1** and **P2** showed deep highest occupied molecular orbital (HOMO) energy levels of -5.50, -5.35 eV, respec-tively which allow delivering high open-circuit voltages (V_{oc}) in bulk heterojunction polymer solar cells (BHJ PSCs). The donor photon energy loss (E_g–eV_{oc}) of **P1** and **P2** are 0.87 and 0.57 which is comparable to the previous reports. BHJ PSCs were fabricated with **P1** and **P2**, and they displayed high V_{oc} of 0.99 and 0.78 V, respectively, with maximum power conversion efficiency of 2.05 and 0.96 % in additive free BHJ PSCs. The polymer field effect transistor mobilities of **P1** and **P2** are 8.0×10^{-3}, 9.2×10^{-5} cm^2/V s, respectively.

✉ Sung-Ho Jin
  shjin@pusan.ac.kr

✉ Jae Wook Lee
  jlee@dau.ac.kr

1   Department of Chemistry Education, Graduate Department of Chemical Materials,
    Institute for Plastic Information and Energy Materials, Pusan National University,
    Busan 609-735, Republic of Korea

2   Department of Energy and Materials Engineering, Dongguk University, 26 Pil-dong,
    3 ga, Jung-gu, Seoul 100-715, South Korea

3   Department of Chemistry, Dong-A University, Busan, Korea

Introduction

Rapid development was encountered in the field of bulk heterojunction polymer solar cells (BHJ PSCs) in the last two decades and realized it as suitable alternative to the silicon based inorganic solar cells [1]. Further the molecular engineering of photo active materials and device optimization gives an impression that it is possible to realize 11 % power conversion efficiency (PCE) for triple junction polymer solar cells and 10 % in the single cell [2, 3]. Encouraging results obtained via benzodithiophene (BDT) based 2D conjugated polymers in the field of PSCs, driven the attention of many research groups towards the synthesis of new 2D conjugated polymers via implanting the new conjugated side chains onto the BDT unit. Desirable features like broad absorption, appropriate highest occupied molecular orbital (HOMO) and lowest unoccupied molecular orbital (LUMO) levels, high hole mobility make them superior candidates for photo active materials in the PSCs [4].

After the first report on alkyl-thiophene substituted BDT based polymers for PSCs, many researchers switch over to replace thiophene side chain with new conjugated side chains to further realize the improved optoelectronic and photovoltaic properties. Eventually it has become an effective strategy to further fine tuning the optoelectronic properties of BDT based 2D conjugated polymers. In this regard several research groups have introduced various kinds of conjugated side chains and synthesized many kinds of copolymers and obtained high PCEs. Among the various kinds of conjugated side chains alkylthiophene, alkylselenophene, alkylfurnanyl, alkyl phenyl, are well optimized and implanted on BDT, the resulted 2D conjugated polymers used as donor materials in BHJ PSCs and obtained high PCEs [5–8]. Further, the 2D conjugated side chains such as bithiophene, alkoxyphenylthiophene, terthiophene substituted BDT based polymers showed deep HOMO energy levels and results higher open-circuit voltage (V_{oc}) for resulting polymer solar cells [9–11]. Thus it is clear that introduction of highly conjugated side chains not only increase the hole mobility but also deepen the HOMO energy level which may help in getting high V_{oc}.

However there are very few reports on bulky conjugated side chain substituted BDT based 2D polymers. In this regard here we try to investigate the effect of introduction of bulky conjugated side chain onto the BDT to further deepen the HOMO energy levels to get the best V_{oc} for BHJ PSCs, since V_{oc} is a key factor which influences the PCE directly. During our course of synthesis and characterization, Renqiang Yang et al. reported terthiophene based bulky side chain linked BDT based polymers and found interesting properties such as deep HOMO energy level and broad absorption spectra etc. [12]. But still the synthesis of new and efficient bulky side chain substituted BDT based polymers are interesting in the field of polymer solar cells to further fine tune the photophysical and photovoltaic properties to get high PCE.

Here we found significant changes in the optoelectronic properties of new 2D conjugated polymers upon introduction of new bulky side chains, especially broad absorption windows, deep HOMO energy levels, and high hole mobilities and these properties would lead to obtain high V_{oc} and short circuit current density (J_{sc}) for resulting PSCs. Particularly **P1** based PSCs delivered a maximum PCE of 2.05 % with a high V_{oc} of 0.99 V nearly $\sim$1 V. The obtained V_{oc} is one of the best V_{oc} reported for additive free PSCs. The polymer field effect transistor mobilities (PFETs) of **P1** and **P2** are 8.0×10^{-3}, 9.2×10^{-5} cm^2/V s, respectively.

Experimental section

Materials and measurements

All chemicals and reagents were purchased from Sigma-Aldrich Chemical Co. Ltd, TCI, and Alfa Aesar, and were used without further purification. ^{1}H and ^{13}C NMR spectra were recorded on a Varian Mercury Plus 300 MHz spectrometer in CDCl$_3$ using tetramethylsilane (TMS) as an internal standard. The UV–Vis absorption spectra were recorded with a JASCO V-570 spectrophotometer at room temperature. Thermal gravimetric analysis (TGA) was carried out on a Mettler Toledo TGA/SDTA 851e analyzer under an N$_2$ atmosphere at a heating rate of 10 °C/min. Polymerization was conducted in CEM focused microwave TM synthesis system (CEM Discover-S). Weight average molecular weight (M_w), number average molecular weight (M_n), and polydispersity index (PDI) were determined against polystyrene as standard by GPC using PL gel 5 μm MLXED-C column on an Agilent 1100 series liquid chromatography system with tetrahydrofuran as an eluent. Cyclic voltammetry measurements were carried out in a 0.1 M solution of tetrabutylammonium tetrafluoroborate in anhydrous acetonitrile at a scan rate of 100 mV/s using CHI 600C potentiostat (CH Instruments); three electrode cell with platinum electrode as the working electrode, Ag/AgCl as the reference electrode and a platinum (Pt) wire as the counter electrode were used. Polymer thin films were coated on Pt electrode and dried before the experiment.

PFETs fabrication and characterization

Glass substrates (Corning Eagle XG) were cleaned sequentially in sonication baths of acetone, isopropanol, and deionized water for 10 min each. The device source/drain (S/D) electrode was patterned by conventional lift-off photolithography processes. Au and Cr (12 nm/2 nm) were used as source and drain metal electrodes. Semiconductors were prepared by dissolving new polymers in anhydrous chloroform (5 mg/1 mL) and the resulting solution was spin coated at 1500 rpm for 60 s, and then thermally annealed at various temperatures such as 150, 200, 250 °C. Poly (methyl methacrylate) (PMMA) 80 mg/mL (Sigma Aldrich, $\sim$120 kM$_w$) in an nBA concentrate solution was spin coated at 2000 rpm for 60 s and then baked at 80 °C for 1 h in glove box (thickness $\sim$500 nm, capacitance: 6.20 nF/cm^2). The transistors were completed by depositing the top gate electrodes (Al) via thermal

evaporation using a metal shadow mask. The electrical characteristics of the PFETs were extracted from the drain current via gate voltage bias or drain voltage bias (channel width (W)/length (L): 1000/20 μm, respectively. Activation energy was extracted from the mobility via a vacuum state probe chamber while decreasing the temperature form 297.15 to 78.15 K in 20 K steps using liquid nitrogen. All measurement was taken using Keithly 4200-SCs semiconductor parameter analyzer connected to glove box probe station.

Fabrication and characterization of the bulk heterojunction polymer solar cells

The ITO and glass substrates that have been used for fabrication were ultrasonically cleaned with detergent, water, acetone, and isopropyl alcohol. Then, a 40 nm thick layer of PEDOT:PSS was coated on the electrodes by spin coating a solution of PEDOT:PSS diluted with isopropyl alcohol with the dilution ratio being 1:2 and annealed at 150 °C for 10 min in oven. A 115 ± 5 nm thick active layer of P1 or P2:PC$_{71}$BM was spin coated using a mixture of polymer:PC$_{71}$BM that was dissolved in o-dichlorobenzene. A 5–10 nm thickness of TiOx spin coated on active layer, and then 100 nm thick Al cathode was deposited via evaporation. The performances of the bulk heterojunction polymer solar cells were measured under simulated AM 1.5G illumination (100 mW/cm^2). The irradiance of the sunlight simulating illumination was calibrated using a standard Si photodiode detector fitted with a KG5 filter. The performance of the bulk heterojunction polymer solar cells were measured using calibrated air mass (AM) 1.5G solar simulator (Oriel® Sol3A™ Class AAA solar simulator, models 94043A) with a light intensity of 100 mW/cm^2 adjusted using a standard PV reference cell (2 cm × 2 cm monocrystalline silicon solar cell, calibrated at NREL, Colorado, USA) and a computer controlled Keithley 2400 source measure unit. The incident photon to current conversion efficiency spectrum was measured using Oriel® IQE-200™ equipped with a 250 W quartz tungsten halogen lamp as the light source and a monochromator, an optical chopper, a lock-in amplifier, and a calibrated silicon photodetector. The thickness of the thin films was measured using a KLA Tencor Alpha-step IQ surface profilometer with an accuracy of ±1 nm. AFM images were acquired with a XE-100 (park system corp.) in tapping mode.

Synthesis of monomers and polymers

Synthesis of 2,3-bis(4-(2-ethylhexyloxy)phenyl)thiophene (1)

2,3 dibromothiophene (3 g, 12.4 mmol) and alkoxyphenylstannate (13.5 g, 27.2 mmol) were dissolved in dry toluene (30 mL) and purged with nitrogen for 20 min then add Pd(PPh$_3$)$_4$ (0.14 g, 0.12 mmol) to the reaction mixture and refluxed for overnight. The reaction mixture was cooled to room temperature and excess solvent was removed, crude product was purified by column chromatography on silica gel with hexane as an eluent to furnish colorless liquid. Yield (43 %). ^{1}H NMR (300 MHz, CDCl$_3$): δ (ppm) 7.47–7.50 (m, 1H), 7.20–7.28 (m, 4H),

7.11–7.13 (m, 1H), 6.96–6.99 (m, 1H), 6.81–6.85 (m, 3H), 3.83–3.90 (m, 4H), 1.70–1.73 (m, 2H), 1.34–1.53 (m, 16H), 0.92–0.97 (m, 12H). ^{13}C NMR (75 MHz, CDCl$_3$): δ (ppm) 158.45, 137.71, 137.00, 133.25, 130.38, 128.85, 127.64, 126.62, 123.20, 114.41, 70.49, 39.36, 30.51, 29.08, 23.83, 23.06, 17.29, 14.13, 11.13. HRMS (ESI) *m/z*: [M + H]$^{+}$ calcd for C$_{32}$H$_{44}$O$_2$S, 492.31; found, 492.30.

Synthesis of 4,8- (bis 2,3-bis(4-(2-ethylhexyloxy)phenyl)thienyl)benzo[1,2-b:4,5-b′]dithiophene (2)

Compound **1** (2.68 g, 5.43 mmol) in dry THF 25 mL and cooled to 0 °C and then n-BuLi (3.2 mL, 8.1 mmol) was added drop wise at 0 °C, then reaction mixture was heated to 50 °C for 1 h and then 4,8-dihydrobenzo[1,2-b:4,-b]dithiophen-4,8-dione (0.6 g, 2.71 mmol) was added to reaction mixture at same temperature and continued the heating for 1 h more and the reaction mixture was cooled to room temperature and then added SnCl$_2$. 2H$_2$O (4.89 g, 21.72 mmol) in 10 mL of (H$_2$O:HCl 7:3 v/v) was added and then stirred for overnight. The reaction mixture was poured into cold water and extracted with methylene chloride and dried over anhydrous MgSO$_4$ and then evaporated the organic layer and resulted crude product was purified by column chromatography on silica gel with (hexane: methylene chloride 9:1 v/v) to furnish yellow colored solid. Yield (21 %). ^{1}H NMR (300 MHz, CDCl$_3$): δ (ppm) 7.84–7.86 (m, 2H), 7.52–7.53 (m, 4H), 7.32–7.36 (m, 8H), 6.85–6.89 (m, 8H), 3.85–3.87 (m, 8H), 1.72–1.74 (m, 4H), 1.35–1.53 (m, 32 H), 0.92–0.97 (m, 24 H). ^{13}C NMR (75 MHz, CDCl$_3$): δ (ppm) 158.95, 158.45, 138.92, 138.55, 137.20, 136.47, 131.36, 130.40, 130.17, 128.64, 127.73, 126.26, 123.70, 114.53, 70.44, 39.39, 30.52, 29.10, 23.85, 23.08, 14.13, 11.15. HRMS (ESI) *m/z*: [M + H]$^{+}$ calcd for C$_{74}$H$_{90}$O$_4$S$_4$, 1171.76; found 1171.75.

Synthesis of 2,6-bis(trimethyltin)- 4,8- (bis 2,3-bis(4-(2-ethylhexyloxy)phenyl)thienyl)benzo[1,2-b:4,5-b′]dithiophene (3)

Compound **2** (0.6 g, 0.51 mmol) in dry THF 20 mL and cooled to −78 °C under N$_2$ atmosphere, *tert*-BuLi (0.9 mL, 1.53 mmol) was added dropwise stirred for 30 min at same temperature and trimethyltin chloride (0.3 g, 1.53 mmol) was added to reaction mixture in one portion and then stirred the reaction mixture at room temperature for overnight. Aqueous sodium carbonate solution was added to the reaction mixture and extracted with methylene chloride and dried over anhydrous MgSO$_4$ to get yellow sticky solid. Yield (84 %). ^{1}H NMR (300 MHz, CDCl$_3$): δ (ppm) 7.88 (m, 2H), 7.57 (m, 2H), 7.34–7.36 (m, 8H), 6.87–6.89 (m, 8H), 3.87 (m, 8H), 1.74 (m, 4H), 1.35–1.55 (m, 32H), 0.94–0.99 (m, 24 H), 0.35–0.54 (m, 18H). ^{13}C NMR (75 MHz, CDCl$_3$): δ (ppm) 158.88, 158.37, 143.25, 142.84, 138.76, 138.43, 138.24, 137.94, 135.90, 133.25, 131.18, 130.25, 128.79, 127.66, 126.34, 123.58, 122.76, 122.00, 114.38, 70.37, 39.38, 30.52, 29.11, 23.85, 23.13, 14.19, 11.19. HRMS (ESI) *m/z*: [M + H]$^{+}$ calcd for C$_{80}$H$_{106}$O$_4$S$_4$Sn$_2$, 1498.50; found 1498.51.

*Synthesis of poly [4,8- (bis 2,3-bis(4-(2-ethylhexyloxy)phenyl)thienyl)benzo [1,2-b:4,5-b′]dithiophene-alt-1,3-di(2-thiophen-5-yl)-5-(2-ethylhexyl)thieno [3,4-c]pyrrole-4,6-dione] (**P1**)*

To a 10 mL of microwave tube compound **3** (0.3 g, 0.2 mmol), A1 (0.11 g, 0.2 mmol), Pd$_2$ (dba)$_3$ (5.4 mg, 2 mol%) and (*o*-tol)$_3$P (16 mg, 16 mol%) were dissolved in anhydrous chlorobenzene 5 mL, and reaction mixture was purged with N$_2$ for 20 min. The microwave tube was placed into the microwave reactor and heated twice at 150 °C for 1 h. After cooling to room temperature reaction mixture was poured into methanol, the resulting precipitate was purified by soxhlet extraction method using methanol, hexane, and acetone and finally chloroform. Finally chloroform fraction was evaporated to get **P1**. Yield (45 %). M_w and PDI are 14,000 g/mol and 1.55. ^{1}H NMR (300 MHz, CDCl$_3$): δ (ppm) 7.73 (br, 2H), 7.49 (br, 2H), 7.34 (br, 10H), 6.85 (br, 10H), 3.83 (br, 8H), 3.52 (br, 2H), 1.71 (br, 5H), 1.33 (br, 40H), 0.92 (br, 30H). Anal. Calcd for C$_{96}$H$_{111}$NO$_6$S$_7$. C, 72.09; H, 7.00; N, 0.88. Found: C, 71.96, H, 6.89, N, 0.82.

Synthesis of poly [4,8- (bis 2,3-bis(4-(2-ethylhexyloxy)phenyl)thienyl) benzo[1,2-b:4,5-b′]dithiophene-alt-2,5-diethylhexyl-3,6-bis(5-thiophen-2-yl) pyrrolo[3,4-c]- pyrrole-1,4-dione] (P2)

To a 10 mL of microwave tube compound **3** (0.3 g, 0.2 mmol), A2 (0.13 g, 0.2 mmol), Pd$_2$ (dba)$_3$ (5.4 mg, 2 mol%) and (*o*-tol)$_3$P (16 mg, 16 mol%) were dissolved in anhydrous chlorobenzene 5 mL, and reaction mixture was purged with N$_2$ for 20 min. The microwave tube was placed into the microwave reactor and heated twice at 150 °C for 1 h. After cooling to room temperature reaction mixture was poured into methanol, resulting precipitate was purified by soxhlet extraction method using methanol, hexane, and acetone and finally chloroform. Finally chloroform fraction was evaporated to get **P2**. Yield (45 %). M_w and PDI are 20,000 g/mol and 1.55. ^{1}H NMR (300 MHz, CDCl$_3$): δ (ppm) 7.99 (br, 2H), 7.58 (br, 2H), 7.52 (br, 4H), 7.33 (br, 8H), 6.87 (br, 8H), 4.04 (br, 8H), 3.86 (br, 4H), 1.73 (br, 6H), 1.34–146 (br, 48H), 0.73–0.93 (br, 36H). Anal. Calcd for C$_{104}$H$_{128}$N$_2$O$_6$S$_6$. C, 73.71; H, 7.61; N, 1.65. Found: C, 73.42, H, 7.45, N, 1.76.

Results and discussion

The synthetic route for the new monomers and polymers are shown in Scheme 1. The new conjugated side (compound **1**) chain was synthesized via Stille coupling of 2,3 dibromothiophene and 4-alkoxy-phneylstannate, further which was implanted on BDT via nucleophilic addition with n-BuLi, and finally distannylation was performed using *tert*-BuLi and trimethyltin chloride to get new monomer D. The polymers **P1** and **P2** were synthesized via microwave assisted Stille coupling reaction. All the monomers were characterized by ^{1}H and ^{13}C NMR spectroscopy and HRMS and the polymers (**P1** and **P2**) were characterized by ^{1}H NMR and elemental analysis. **P1** and **P2** are readily soluble in common organic solvents like
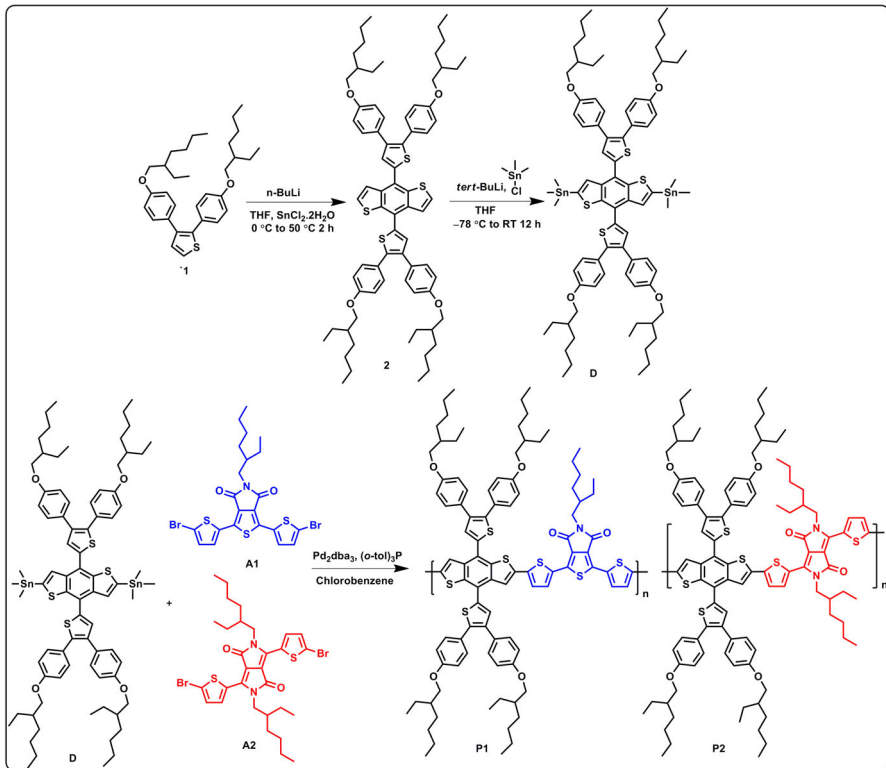
Scheme 1 Synthetic route for monomers and polymers

chloroform, THF, chlorobenzene, 1,2-dichlorobenzene. TGA was performed to investigate the thermal stability of the new polymers and the corresponding thermo grams are shown in Fig. 1 the decomposition temperatures (T_d) of the **P1** and **P2** are 437, 430 °C, respectively indicates that the synthesized polymers posses high thermal stability for optoelectronic applications.

Optical properties

The UV–Vis absorption spectra of **P1** and **P2** were measured in dilute chloroform solution and film states as represents in Fig. 2, both **P1** and **P2** showed broad absorption patterns from 300 to 650 nm, 300 to 900 nm, respectively with two distinct absorption peaks such as π–π* transition between polymer backbones and intramolecular charge transfer (ICT) which implies charge transfer between electron rich and electron deficient units. **P1** shows bathochrmoic shift in film state compared to solution state, whereas **P2** does not show any change in film state compared to solution which might be due to rigid structure of **P2**. The absorption maxima of the **P1** and **P2** are 584, 751 nm and 592, 741 nm in solution and film state, respectively. The absorption spectra of **P1** and **P2** shows vibronic shoulders at
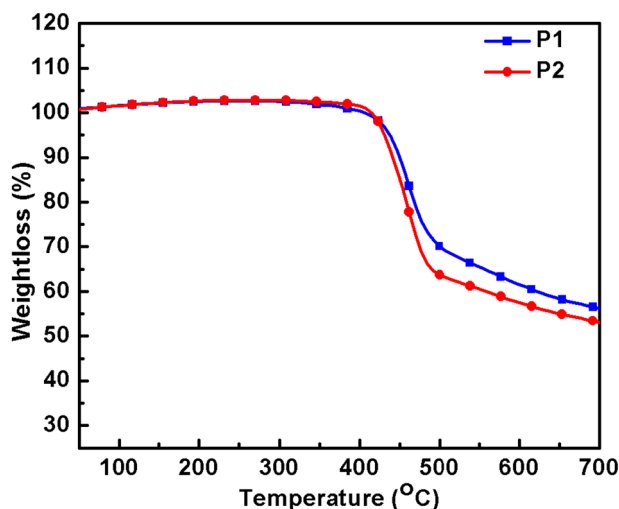
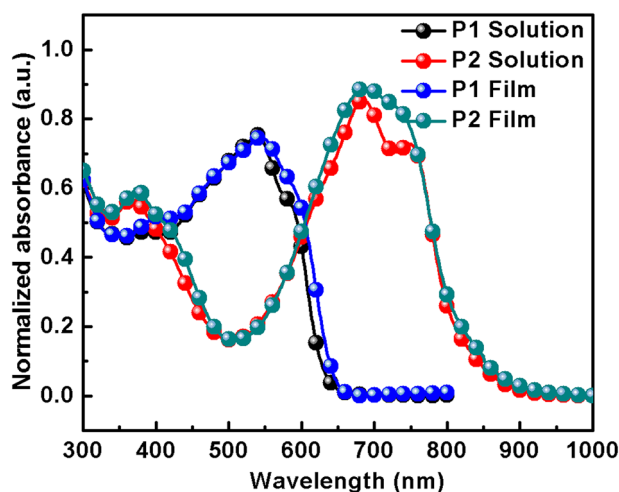**Fig. 1** TGA curves of **P1** and **P2**

Fig. 2 UV–Vis absorption spectra of **P1** and **P2** in chloroform solution and film state

585–590 nm and 745–750 nm, respectively indicates π–π stacking polymers. Both **P1** and **P2** displayed better ICT bands compared to their π–π* bands. The optical band gaps of the polymers are 1.89, 1.38 eV, respectively which were calculated from absorption edges of film state spectra. The molar extinction coefficients of the **P1** and **P2** are around (6×10^4; 8×10^4 M^{-1} cm^{-1}), respectively indicates that they can harvest good amount of sunlight. The photophysical properties of the polymers are shown in the Table 1.

**Table 1** Optical and electrochemical properties of **P1** and **P2**

Polymer	Solution λ_{max} (nm)[a]	Film λ_{max} (nm)[b]	Film λ_{max} (nm)[c]	E_g^{opt} (eV)[d]	HOMO (eV)	LUMO (eV)
P1	539, 584	546, 592	666	1.86	5.50	3.64
P2	683, 751	688, 741	918	1.35	5.35	3.97

[a] Absorption maxima measured from UV–Vis absorption spectrum in chloroform

[b] Absorption maxima measured from UV–Vis absorption spectrum in thin film state

[c] The onset of the film state absorption spectra

[d] Estimated from the onset of the absorption in thin films ($E_g^{opt} = 1240/\lambda_{onset}$)
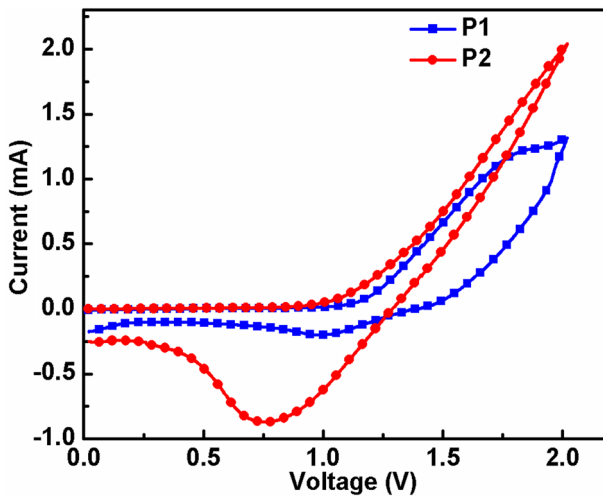
Fig. 3 Cyclic voltammograms of **P1** and **P2**

Electrochemical properties

HOMO and LUMO energy levels of **P1** and **P2** were determined from the cyclic voltammetry and resulting voltammograms are shown in Fig. 3, the onset oxidation potentials of **P1** and **P2** are 1.15 and 1 V, respectively. The HOMO levels of the polymer films were estimated from the cyclic voltammograms, using the equation HOMO $= -(E_{onset}^{ox} - $ ferrocene$_{onset}) - 4.8$ eV, where E_{ox} is the onset oxidation potential relative to the ferrocene as standard material (0.45 V). Further the LUMO energy levels were calculated from E_g^{opt} and HOMO energy levels obtained from cyclic voltammetry [13]. The HOMO energy levels of the **P1** and **P2** are -5.50 and -5.35 eV which are very deep and could able to display high V_{oc} in BHJ PSCs, since V_{oc} is highly related to HOMO of donor and LUMO of acceptor (PC$_{71}$BM). All the polymers are highly air stable since their HOMO energy levels are below the air oxidation threshold limit (-5.2 eV). Here we also observed that **P1**, **P2** attained

deeper HOMO energy levels than regular TPD, DPP based polymers this attributed to the new bulky conjugated side chains attached to the BDT, and this can be considered as a new method to reducing the HOMO energy level. The LUMO energy levels are −3.64 and −3.97 eV which can provide enough LUMO level offset between the polymer and $PC_{71}BM$ for good exciton dissociation at the donor/acceptor interface.

PFETs characteristics

Top gate, bottom contact PFETs with **P1** and **P2** were fabricated on glass substrate with a PMMA gate dielectric layer. Both the polymers delivered prominent field effect hole mobilities indicating that they posses p-type behavior which is useful characteristic for polymer solar cells as donor materials. The new conjugated polymers were annealed at various temperatures such as 150, 200, 250 °C for 30 min to improve the PFET performances. Figure 4 shows the typical transfer and out curves of PFETs that were annealed at 150, 200, 250 °C, respectively and the resulting hole mobilities are shown in Table 2. The hole mobilities of **P1** and **P2** were improved after increasing the annealing temperatures 150–250 °C. The **P1** showed higher hole mobilities compared to the **P2**, it can be expected that **P1** can deliver better photovoltaic parameters than **P2**. The hole mobilities of the **P1** are 1.6×10^{-4} (150 °C), 8.3×10^{-4} (200 °C), 8.0×10^{-3} cm^2/V s (250 °C) where as **P2** showed 3.0×10^{-6} (150 °C), 8.8×10^{-5} (200 °C), 9.2×10^{-5} cm^2/V s (250 °C).
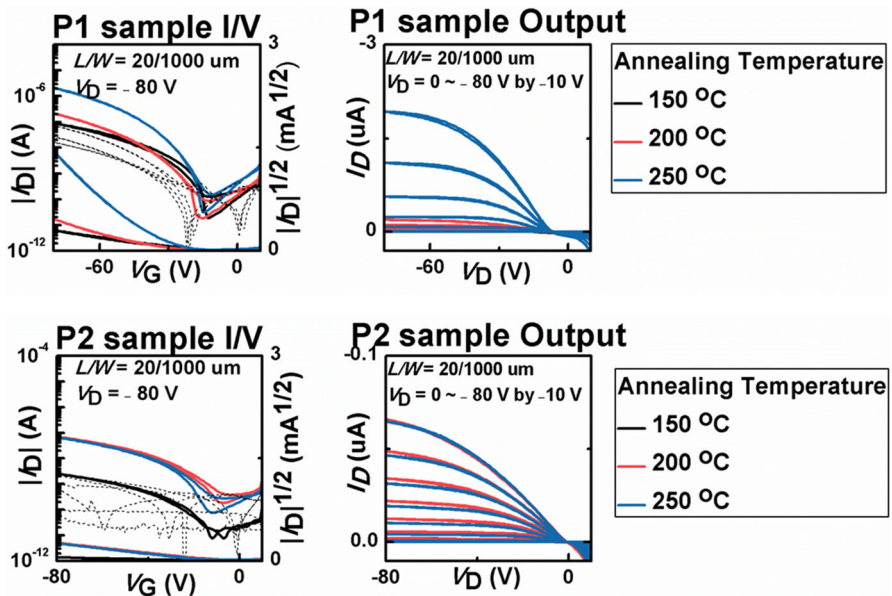

Fig. 4 Transfer characteristics of PFETs based on **P1** and **P2**

Table 2 Transfer characteristics of **P1** and **P2**

Polymer	Annealing temperature (°C)	μ sat cm^2/V s	V_{TH} (V)	S.S (V/dec.)
P1	150	1.6×10^{-4}	−21.23	−2.4
P1	200	8.3×10^{-4}	−39.35	−2.26
P1	250	8.0×10^{-3}	−39.12	−2.39
P2	150	3.0×10^{-6}	−7.44	−5.66
P2	200	8.8×10^{-5}	−9.25	−9.35
P2	250	9.2×10^{-5}	−13.5	−7.27

Photovoltaic properties

BHJ PSCs were made in conventional device structure (ITO/PEDOT:PSS/P1-P2:PC$_{71}$BM/TiOx/Al) with new polymers to understand the effect of new bulky side chains on photovoltaic properties. Here we used TiOx as buffer layer between active layer and metal electrode, since it can act as optical spacer; efficient electron transporting or hole blocking layer, and it can also act as shielding layer for active layer by protecting from moisture and oxygen and can improve the PCE of resulting PSCs. The current density–voltage (J–V) curves for **P1** and **P2** based devices with various blending ratios were shown in Fig. 5, and the resulting photovoltaic properties such as J_{sc}, V_{oc}, fill factor (FF), PCEs are shown in Table 3. It is fact that blending ratio is very important in getting suitable nanoscale morphology for active layer, for this we have tried various ratios of polymer to PC$_{71}$BM such as 1:1, 1:2, 1:3. Among the three ratios 1:3 ratio has given the best photovoltaic properties for the **P1** based PSCs whereas in case of **P2** based PSCs opted 1:2, and optimized thickness of active layers are around 115 ± 5 nm. In case of **P1** based devices showed the improvement in photovoltaic properties from 1:1 to 1:3 was observed and further increment in PC$_{71}$BM content resulted poor device performance, whereas in case of **P2** based devices from 1:1 to 1:2 there was little improvement where as further increment in PC$_{71}$BM content resulted in poor device parameters.

P1 and **P2** based PSCs showed maximum PCE of 2.05 % with V_{oc} of 0.99 V, FF of 46.59 %, J_{sc} of 4.45 mA/cm^2 in 1:3 blending ratio, where as in case of **P2** maximum PCE of 0.96 % with V_{oc} of 0.78 V, FF of 41.75, J_{sc} of 2.91 mA/cm^2 was realized. Both **P1** and **P2** based devices displayed high V_{oc} values of 0.99 and 0.78 V, these high V_{oc} values can be attributed to its deep HOMO energy levels attained via introduction of new bulky side chains. Even though **P1** based devices showed high J_{sc} in 1:2 composition, the devices with polymer:PC$_{71}$BM composition of 1:3 gave better PCE due to high V_{oc} and FF. From this it is clear that these new bulky side chains can significantly reduce the HOMO of donor polymers and this could have facilitated to enhance V_{oc} for the BHJ PSCs, which is one of the key parameter which can directly improve the PCE. Here we also calculated the donor photon energy loss E_g-eV_{oc} for **P1** and **P2** are about 0.87 and 0.57 which is in the range of previous reports with V_{oc} of 0.99 and 0.78 V and with E_g of 1.86 and 1.35 eV.
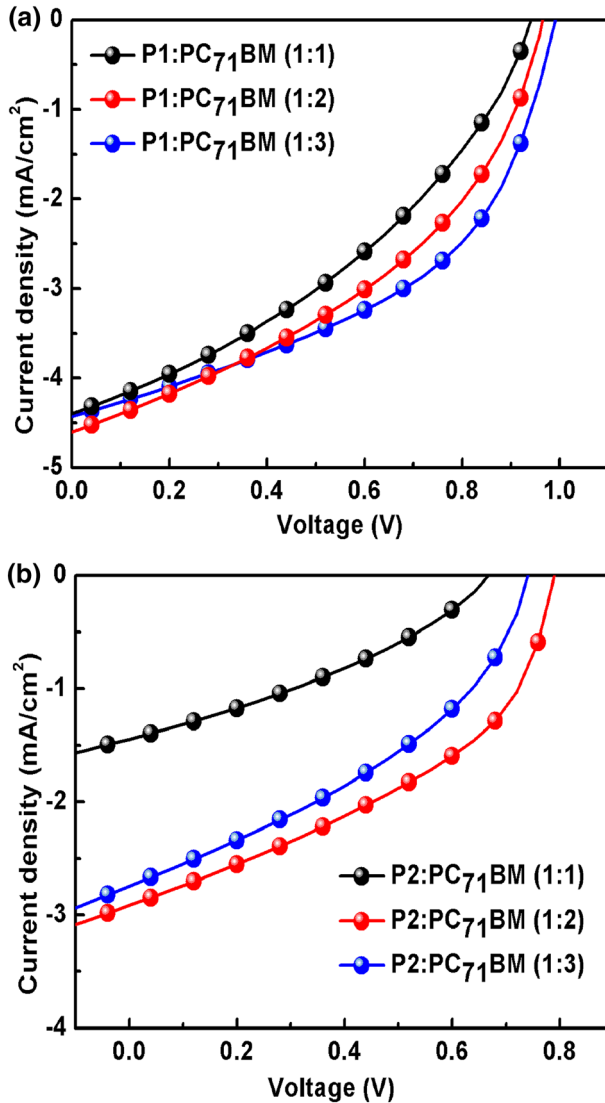
Fig. 5 *J–V* curves of **P1** and **P2** based additive free BHJ PSCs

The accuracy of photovoltaic parameters can be confirmed by external quantum efficiency (EQE) of the PSCs, the EQE curves of **P1** and **P2** based additive free PSCs can be seen in Fig. 6. Both the **P1** and **P2** PSCs showed good response from 300 to 700 nm and 300 to 900 nm, respectively. **P1**, **P2** based devices with various ratio showed broad EQE response which is correlated with their J_{sc}. The EQE values of **P1** based devices showed up to 35 % whereas **P2** showed maximum EQE of 25 % which is well correlated with higher PCE of **P1**. The calculated J_{sc} values of **P1** and **P2** based devices from integration of the EQE spectra were well

Table 3 Photovoltaic properties of **P1**, **P2** based BHJ PSCs

Polymer	Polymer:PC$_{71}$BM	J_{sc} (mA/cm^2)	V_{oc} (V)	FF (%)	PCE (%)
P1	1:1	4.39	0.94	37.54	1.55
P1	1:2	4.60	0.96	40.97	1.82
P1	1:3	4.45	0.99	46.59	2.05
P2	1:1	1.44	0.66	34.13	0.32
P2	1:2	2.91	0.78	41.75	0.96
P2	1:3	2.74	0.74	38.36	0.77
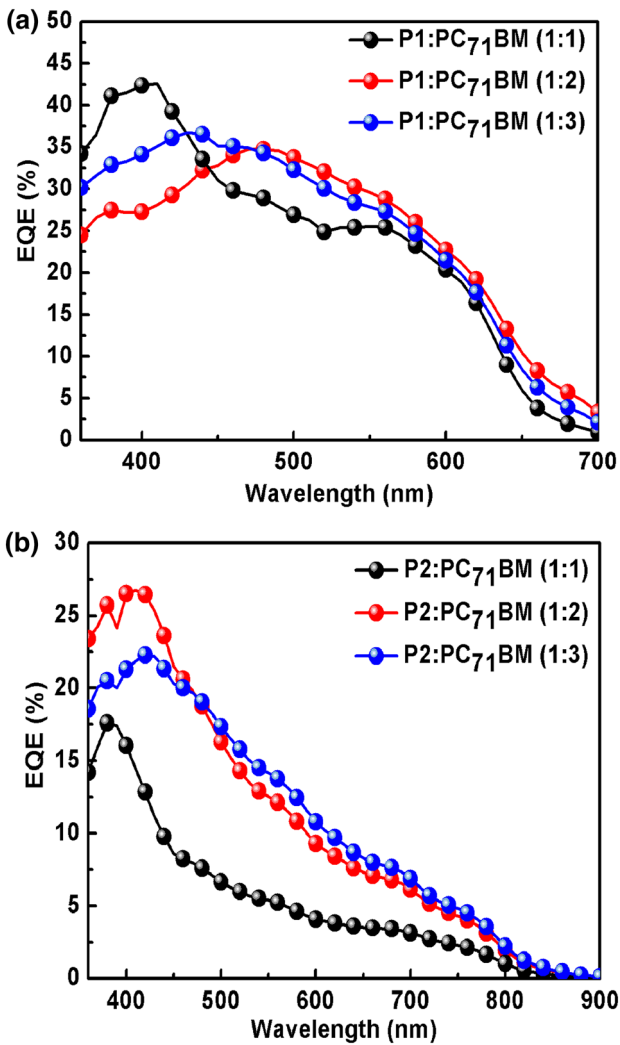
Fig. 6 EQE spectra of **P1** and **P2** based additive free BHJ PSCs

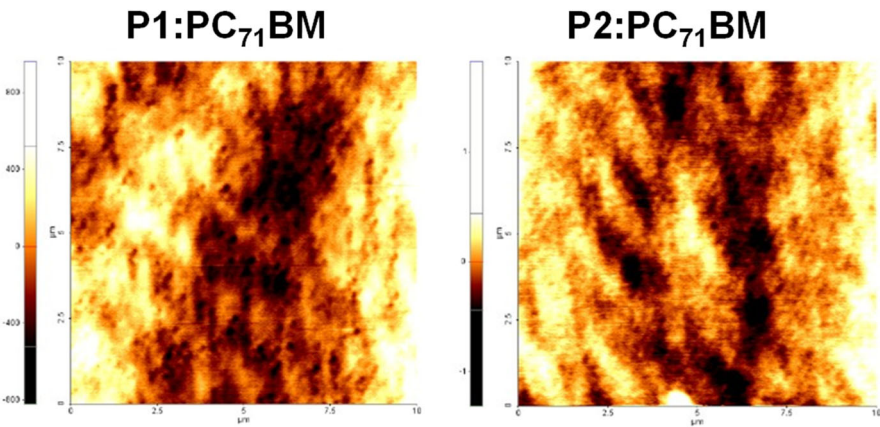## P1:PC$_{71}$BM   P2:PC$_{71}$BM

Fig. 7 AFM images of **P1**, **P2** active layers

consistent with J_{sc} obtained from the J–V measurements with the common error of 5–10 %.

Morphological properties

Understanding the nanoscale morphology of active layer is very important in BHJ PSCs since it plays vital role in deciding the performance of the BHJ PSCs. Active layer morphology of new polymer blends was studied by tapping mode atomic force microscopy (AFM) and the AFM images are shown in Fig. 7, and the root mean square roughness (rms) of P1:PC$_{71}$BM and P2:PC$_{71}$BM was found to be 0.26 and 0.22 nm, respectively. Both the active layers showed smooth surface roughness compared to the previously reported hyper conjugated polymers. It is fact that good phase separation between the polymer and PC$_{71}$BM could able to make effective nanoscale morphology to get proper charge transport towards respective electrodes. The excess smooth morphology of **P1** and **P2** active layers might have created by homogenous separation of the polymer and fullerene, which might lead to insufficient phase separation poor charge transport in blends leads to poor device performance. The poor active layer morphology of **P2** further explains weak EQE response values and the J_{sc} of **P2** devices based on are miserably low which ultimately results poor PCE for **P2** even though it possess narrow band gap than **P1**.

Conclusions

The introduction of new bulk side chains of BDT unit has brought significant changes in optoelectronic properties such as broad absorption profiles, and deep HOMO energy levels of 2D-conjugated polymers which could lead to attain high V_{oc} for **P1** and **P2** based PSCs. Further new conjugated polymers showed notable changes in photovoltaic properties such as high V_{oc} of 0.99 V nearly 1 and

0.78 V with maximum PCE of 2.05, 0.96 % for additive free **P1**, **P2** based BHJ PSCs. **P1** and **P2** also showed good PFET characteristics with hole mobilities of 8.0×10^{-3} and 9.0×10^{-4} cm^2/V s, which are well concured with photovoltaic properties of **P1** and **P2**. Further improvement in device performance can be possible via further device optimization and also by addition of external additives and also changing the device architectures. Overall, this work provides a new and effective method to get deep HOMO levels for BDT based polymers, which can be useful for design of conjugated polymers with high V_{oc} which results in getting high performance photovoltaic polymers.

References

1. Cheng YJ, Yang SH, Hsu CS (2009) Synthesis of conjugated polymers for organic solar cell applications. Chem Rev 109:5868
2. Chen CC, Chang WH, Yoshimura K, Ohya K, You J, Gao J, Hong Z, Yong Y (2014) An efficient triple-junction polymer solar cell having a power conversion efficiency exceeding 11 %. Adv Mater 26:5670
3. He Z, Xiao B, Liu F, Wu H, Yang Y, Xiao S, Wang C, Russel TP, Cao Y (2015) Single-junction polymer solar cells with high efficiency and photovoltage. Nat Photonics 9:174
4. Ye L, Zhang S, Huo L, Zhang M, Hou J (2014) Molecular design toward highly efficient photovoltaic polymers based on two-dimensional conjugated benzodithiophene. Acc Chem Res 47:1595
5. Huo L, Zhang S, Guo X, Xu F, Li Y, Hou J (2011) Replacing alkoxy groups with alkylthienyl groups: a feasible approach to improve the properties of photovoltaic polymers. Angew Chem Int Ed 50:9697
6. Kranthiraja K, Gunasekar K, Cho W, Park YG, Lee JY, Shin Y, Kang IN, Song M, Chae KH, Kim BS, Jin SH (2015) Influential effects of π-spacers, alkyl side chains, and various processing conditions on the photovoltaic properties of alkylselenyl substituted benzodithiophene based polymers. J Mater Chem C 3:796
7. Wang Y, Yang F, Liu Y, Peng R, Chen S, Ge Z (2013) New alkylfuranyl-substitued benzo[1,2-b:4,5-b′]dithiophene based donor-acceptor polymers for highly efficient solar cells. Macromolecules 46:1368
8. Dou L, Gao J, Richard E, You J, Chen CC, Cha KC, He Y, Li G, Yang Y (2012) Systematic investigation of benzodithiophene-and diketopyrrolopyrrole-based low bandgap polymers designed for single junction and tandem polymer solar cells. J Am Chem Soc 134:10071
9. Kularatne RS, Sista P, Nquyen HQ, Bhatt MP, Biewer MC, Stefan MC (2012) Donor–acceptor semiconducting polymers containing benzodithiophene with bithienyl subsituents. Macromolecules 45:7855
10. Kranthiraja K, Gunasekar K, Cho W, Song M, Park YG, Lee JY, Shin Y, Kang IN, Kim A, Kim H, Kim BS, Jin SH (2014) Alkoxyphenylthiophene linked benzodithiophene based medium band gap polymers for organic photovoltaics: efficiency improvement upon methanol treatment depends on the planarity of backbone. Macromolecules 47:7060
11. Liu Q, Bao X, Wen S, Du Z, Han L, Zhu D, Chen Y, Sun M, Yang R (2014) Hyperconjugated side chained benzodithiophene and 4,7-di-2thienyl-2,1,3-benzodithiadiazole based polymer for solar cells. Polym Chem 5:2076
12. Liu Q, Bao X, Han L, Gu C, Qiu M, Du Z, Sheng R, Sun M, Yang R (2015) Improved open-circuit voltage of benzodithiophene based polymer solar cells using bulky terthiophene side group. Sol Energ Mat Sol Cells 138:26
13. Cheon YR, Kim YJ, Ha JJ, Kim MJ, Park CE, Kim YH (2014) TPD-based copolymers with strong interchain aggregation and high hole mobility for efficient bulk heterojunction solar cells. Macromolecules 47:8570